ADVANCED MATERIALS INTERFACES
www.advmatinterfaces.de

Polysilazane-Based Coatings with Anti-Adherent Properties for Easy Release of Plastics and Composites from Metal Molds

*Gilvan Barroso, Michael Döring, Alexander Horcher, Andreas Kienzle, and Günter Motz**

Polysilazanes are excellent coating materials, because of their self-crosslinking in air at low temperatures, high chemical and thermal stability, elevated hardness, and excellent adhesion to many different substrates. Therefore, coatings of two chemically different polysilazanes (crosslinked Durazane 1800 (HTTS)/perhydropolysilazane (PHPS)) are deposited by either dip or spray coating and crosslinked at 200 or 300 °C in air to investigate the chemical composition, surface energy, and coating adhesion in dependency on the precursor type and crosslinking temperature. The silazane HTTS possesses a higher amount of nonpolar organic groups resulting in a lower surface free energy. The anti-adherence properties are investigated by using a phenolic resin via pull-off adhesion, which is slightly reduced from 13 MPa for uncoated aluminum to less than 10 MPa for HTTS coated substrates. The addition of different amounts of poly(tetrafluoroethylene) (PTFE) particles causes a remarkable reduction of the surface free energy leading to a strongly reduced pull-off adhesion of less than 4 MPa of the phenolic resin from the HTTS/PTFE coated substrates. The anti-adherent properties remain even after repeated pull-off tests. Because of the excellent properties, the HTTS/PTFE coatings are a very suitable system for easy mold release of plastic parts from metal molds and to replace commercial nonstick PTFE coatings.

1. Introduction

Polysilazanes are silicon-based polymers containing alternating silicon and nitrogen atoms in their backbone. When thermally treated at temperatures above 400 °C, in a process generally called pyrolysis, these materials can be converted into ceramics, such as Si_3N_4, SiON, SiCN, SiCNO, or SiC depending on the chemical composition of the polymer and on the pyrolysis atmosphere.[1] Owing to this capability, polysilazanes are used as precursors in the processing of ceramic coatings by the polymer-derived ceramic (PDC) route.[2]

However, polysilazanes have outstanding properties also in polymeric—or preceramic—stage. Compared to most organic polymers, polysilazanes have enhanced thermal and chemical stability, and higher hardness.[3] Also the coating adhesion is usually stronger than of typical organic coatings, attributed to reactions with −OH groups, present at the surface of most materials, leading to chemical bonding between coating and substrate.[4,5] Suitable polysilazanes for coating applications are either liquids or soluble solids. Thus, deposition in liquid phase by simple methods, such as dip, spin, and spray coating techniques are possible. After deposition, a crosslinking process generates a thermoset material with enhanced thermal, mechanical and chemical stability. Although crosslinking of polysilazanes can be induced by different methods, such as by a reactive atmosphere[6,7] and by UV radiation,[8,9] thermal crosslinking at temperatures between 150 and 400 °C[1,10] is the most common procedure. In this case, the substrates must have a sufficient thermal stability to withstand the thermal treatment without detrimental effects.

Polysilazane-based coatings have been developed for a large variety of applications at temperatures ranging from below 0 to 1500 °C and beyond.[2] These coatings can modify surface properties of common structural materials to increase the mechanical and chemical resistance of the system[11–17] or to tailor specific properties, such as thermal conductivity,[18] biocompatibility,[19] wettability,[20] permeability,[9,21] antibacterial,[22] antifouling,[23] and optical properties.[10] Another application of polysilazane-based coatings—from the best of our knowledge, until now unexplored—is anti-adherence. Such coatings could be used, for example, for the processing of plastic and composite parts, such as carbon-fiber reinforced plastics (CFRP). Due to the increasing necessity of reducing weight of structures without sacrificing mechanical performance, industries, such as aerospace, automotive, and sport articles, have been continuously extending the use of plastics and composites. Common processes of plastic parts are injection molding and resin transfer molding (RTM), usually employing metallic molds. Especially when pressure and heat are required for the shaping process, adhesion of the organic resins to the molds can lead to a difficult demolding, which may cause damage of parts and molds.[24] Moreover, the removal of resin residues

Dr. G. Barroso, M. Döring, A. Horcher, Dr. G. Motz
Ceramic Materials Engineering (CME)
University of Bayreuth
Bayreuth 95440, Germany
E-mail: guenter.motz@uni-bayreuth.de
Dr. A. Kienzle
SGL Carbon GmbH
Werner-von-Siemens-Straße 18, Meitingen 86405, Germany
The ORCID identification number(s) for the author(s) of this article can be found under https://doi.org/10.1002/admi.201901952.

DOI: 10.1002/admi.201901952

from the molds, required before a new pressing procedure can be started, increases process time and production costs.[25]

Several types of coatings with nonstick properties have been developed, mostly based on organic polymers. The best known example of such coatings are poly(tetrafluoroethylene) (PTFE)-based layers applied on kitchen utensils, such as frying pans.[26] PTFE stands out not only because of its low surface energy and coefficient of friction, but also due to its high thermal and chemical stability when compared to other organic polymers.[27,28] Despite the high wear resistance resulting from their self-lubricating properties, these coatings suffer from a limited scratch resistance because of their relatively low hardness.[29] Another problem is the application of PTFE coating. Usually, fine powdered PTFE is forced into a mold under high pressure and subsequently annealed up to days at higher temperatures to form a homogeneous layer. Often, it is also necessary sandblast the metal to generate a rough surface to allow for a physical adhesion of the primer PTFE coat by mechanical interlocking. After a thermal treatment, a finishing layer of PTFE is applied onto the primed surface followed by a further thermal treatment. Other types of anti-adherent surfaces include Al–Cu–Fe–Cr quasicrystalline coatings[30] and Ni–PTFE/Ni–P–PTFE composite layers,[31,32] which require much more complicated processes. More simple approaches include the use of fluoroalkylsilane[33] and polysiloxane-based (silicone) coatings.[34] Despite the very low surface energy provided by fluoroakylsilanes, these coatings are very thin, and thus extremely sensitive to the quality of the substrate's surface.[24] Polysiloxane-based coatings, in contrast, result in robust coatings, which, however, have a reduced thermal stability and a slower rate of crosslinking, when compared to polysilazanes.[10,35] Also liquid release agents are available. These agents, however, can contaminate the surface of the shaped part, which may have a negative effect on further processing steps, requiring a posterior cleaning of the shaped part.[36] Moreover, they require frequent reapplication, which increases process time and costs.

In this work, we developed polysilazane-based coating systems containing different fillers applied onto aluminum substrates by a simple process, aiming at anti-adherent properties for easy release of CFRP parts, for example, from aluminum molds. Although the developed systems can be applied in different plastic molding process, coating development was focused on the processing of ceramic brakes. In this case, the CFRP discs are produced from short carbon fibers and a phenolic resin by warm compression molding. During this process, the resin may adhere strongly to the aluminum mold, causing the damage of the shaped part during demolding and leading to a large scrap rate. Furthermore, the CFRP mass is very abrasive, so that the surface of the aluminum mold becomes very rough over time, further improving the adhesion of the resin. After shaping and hardening, the CFRP discs are pyrolyzed, whereby the phenolic resin is converted into a porous carbon material. In a following step, the porous carbon bodies are infiltrated with molten silicon—liquid silicon infiltration (LSI) process—at high temperatures under reduced pressure, inducing a reaction between silicon and carbon, forming carbon fiber reinforced SiC with some residual carbon in the matrix (C/C–SiC). Another objective of the work was the development of a test methodology for a reproducible and application-oriented characterization of the anti-adherent properties of different coatings. The developed coatings were investigated regarding adhesion of a phenolic resin, adhesion of the coatings to the substrates, microstructure, chemical composition, surface energy, and durability of the anti-adherent properties.

2. Experimental Section

2.1. Materials

Two silazanes were selected for the development of coatings with anti-adherent properties: perhydropolysilazane Durazane 2250 (PHPS) and the organosilazane Durazane 1800 (both from Merck KGaA, Germany). The first is an inorganic polymer, containing only silicon, nitrogen, and hydrogen, whereas the second is an oligomer containing carbon in the form of methyl and vinyl side groups attached to the —Si—N— backbone.[18] Due to its high reactivity with moisture, PHPS is commercialized as a 20 wt% solution in di-*n*-butyl ether. Durazane 1800, in contrast, is available as a pure liquid. To avoid the evaporation of species with low molecular weight during thermal crosslinking, a simple pre-crosslinking of Durazane 1800 using tetra-*n*-butyl ammonium fluoride (TBAF, Alfa Aesar, Germany) as catalyst was carried out according to Flores et al.[37] After this pre-crosslinking, Durazane 1800 becomes a solid polymer known as HTTS, which is still easily soluble in nonpolar solvents, such as di-*n*-butyl ether or toluene. In this work, HTTS was diluted to a concentration of 20 wt% in di-*n*-butyl ether (99+% purity, Acros Organics BVBA, Belgium) to obtain low viscous solutions, suitable for coating deposition. To reduce the onset temperature of the crosslinking reactions of HTTS, 3 wt% of dicumyl peroxide (DCP, Sigma-Aldrich Chemie GmbH, Germany), which acts as an initiator for the crosslinking reactions, was added to the coating solution.

Three different fillers were investigated: graphite powder (d_{50} = 5 µm, SynCarb DLB-LB, ChemSys GmbH, Germany), hexagonal boron nitride (h-BN, d_{50} = 1 µm, HeBoFill 410, Henze BNP AG, Germany), and PTFE (d_{50} = 1 µm, Sigma-Aldrich Chemie GmbH, Germany). Di-*n*-butyl ether was used to adjust the viscosity of the polymer solutions and to prepare filler suspensions. DISPERBYK 2070 (BYK-Chemie GmbH, Germany) was used as dispersant for the filler particles and to stabilize the suspensions.

Aluminum plates with dimensions of 50 mm × 50 mm with thickness of 10 mm, composed of the same material used for the manufacturing of industrial pressing molds, were provided by SGL Carbon GmbH (Germany). A phenolic resin typically used for production of CFRP composite preforms for ceramic brakes, was used for adhesion tests. This solid resin was supplied as a powder with a melting temperature around 70 °C and hardening temperature around 170 °C.

2.2. Preparation of Coatings

As mentioned, coating solutions containing 20 wt% HTTS in di-*n*-butyl ether were prepared by dissolving the solid material.

After complete dissolution, 3 wt% of DCP (regarding the amount of silazane) was added and dissolved by magnetic stirring. PHPS was used as received (20 wt% solution in di-*n*-butyl ether, without initiator).

Filler suspensions were prepared by dissolving DISPERBYK 2070 (5 wt% of the amount of filler) in di-*n*-butyl ether by stirring. After complete dissolution, the respective filler powders were added and the suspension was magnetically stirred for about 24 h to ensure a sufficient dispersion of the particles. At last, the necessary amount of silazane was added to the suspensions. Filler amounts varying in the range of 5–70 vol% were investigated.

Before coating deposition, the surface of the aluminum substrates was ground with SiC paper grit 1200, to ensure a homogeneous, defect-free, and reproducible surface quality. The paper grit was empirically selected to obtain a surface sufficiently rough to improve adhesion of the coatings to the substrate. Afterward, the surface was cleaned by ultrasonication using acetone.

Deposition of the coatings was carried out using two different methods. Unfilled silazane coatings were deposited by dip coating using automatic equipment (RDC 15, Bungard Elektronik GmbH & Co. KG, Germany) with a hoisting speed of 5 mm s^{-1}. The suspensions were deposited using a semiautomatic spray equipment (Isel Germany AG, Germany) with a spray unit model 780S (Nordson Deutschland GmbH, Germany) and a homemade control system.

Due to the low melting temperature of aluminum and its alloys, the temperature for crosslinking of the deposited coatings must be kept low, to avoid damage, deformation, and degradation of the properties of the substrates. Moreover, since hardening of the phenolic resin takes place at 170 °C, coatings must be previously treated at least at this temperature, to avoid changes of the coating properties by further crosslinking reactions during application, which could influence the quality of the CFRP products. Hence, two temperatures for the curing of the coatings were investigated: 200 and 300 °C. Crosslinking was performed in a chamber furnace (B 150, Nabertherm GmbH, Germany) with natural air atmosphere. The temperature was raised with a heating rate of 5 K min^{-1}, followed by a holding step of 1 h at the maximum temperature. Cooling of the samples was performed naturally within the closed furnace.

2.3. Characterization Methods

The degree of crosslinking of the silazane-based coatings was analyzed by Fourier transform infrared (FTIR) spectroscopy in attenuated total reflectance (ATR) mode (Tensor 27, Bruker Optik GmbH, Germany).

Surface microstructure of the developed coatings was analyzed by scanning electron microscopy (SEM) (Zeiss Gemini Sigma 300 VP, Carl Zeiss AG, Germany). Roughness of substrates and coatings was quantified by stylus profilometry (Garant Perthometer H2, Hoffmann Group GmbH & Co. KG, Germany). Adhesion of the coatings to the substrate was evaluated by cross-cut tape test (DIN EN ISO 2409) using a test kit ZCC 2087 (Zehntner GmbH, Germany). The evaluation of the test area was carried out by optical microscopy (Stemi SV 11, Carl Zeiss AG, Germany).

Surface free energy (SFE, γ_s) of substrate and coatings was determined by contact angle (CA) analysis (DSA 25E, Krüss GmbH, Germany) using the sessile drop method. The contact angle of the surfaces with distilled water and diiodomethane (99%, stabilized, Thermo Fisher (Kandel) GmbH, Germany) was measured in four different areas of the samples. All samples were cleaned with isopropanol and a cloth, and dried with clean compressed air prior to the measurements. Droplets with a volume of ≈2 µL were generated by an electronic dosing unit. The measurements were performed about 3 s after deposition of the droplet onto the surface. Droplet contour was fitted using the ellipse method. The OWRK model was employed to calculate the SFE of the surfaces, including the respective dispersive and polar components, based on the measured contact angle values and the surface tension of the liquids (γ_l). The input values for the properties of water were $\gamma_l = 72.80$ mN m^{-1}, $\gamma_l^{disp} = 21.80$ mN m^{-1}, $\gamma_l^{pol} = 51.00$ mN m^{-1}; and for diiodomethane $\gamma_l = 50.80$ mN m^{-1}, $\gamma_l^{disp} = 50.80$ mN m^{-1}, $\gamma_l^{pol} = 0.00$ mN m^{-1}.

To characterize adhesion of the phenolic resin to coated and uncoated substrates, a methodology was developed based on pull-off tests (ASTM D4541). In this method, an aluminum dolly was bonded to the surface of the coating with a strong epoxy adhesive and was perpendicularly pulled off. The testing equipment (PosiTest AT-A, DeFelsko Corp., USA) measures the tension necessary to detach the dolly from the surface. In this study, the typical epoxy adhesive was substituted by the phenolic resin used for the manufacturing of CFRP discs for ceramic brakes. The procedures for sample preparation were designed to simulate a real application and consisted of five steps (**Figure 1**):

1. A PTFE ring with outer diameter of 22 mm, inner diameter of 14 mm, and thickness of 0.5 mm was placed onto the uncoated or coated aluminum substrates. This ring had the function of containing the molten resin, avoiding spreading during the following steps.
2. A defined amount of resin (0.1 g) was placed and homogeneously distributed inside the PTFE ring.
3. The aluminum substrate was placed onto a hot plate (100 °C), where the solid resin melted.
4. The surface of the dolly (circular area with diameter of 20 mm) was roughened to improve adhesion and the dolly was placed onto the molten resin, fixated, and pressed by clamps.
5. The assembly was placed in the furnace, where the temperature was increased to 170 °C with a heating rate of 3 K min^{-1}, temperature at which the assembly was held for 30 min. After natural cooling, the clamps were removed.

Before the measurements, the diameter of the resulting circular test area of 14 mm (corresponding to inner diameter of the PTFE ring) and a pull rate of 0.4 MPa s^{-1} were set in the equipment, after which the measurements began.

Durability tests were performed by repeating the pull-off test five times on the same area of each sample. The variation of the adhesion strength was used as criterion to evaluate the durability of the systems.

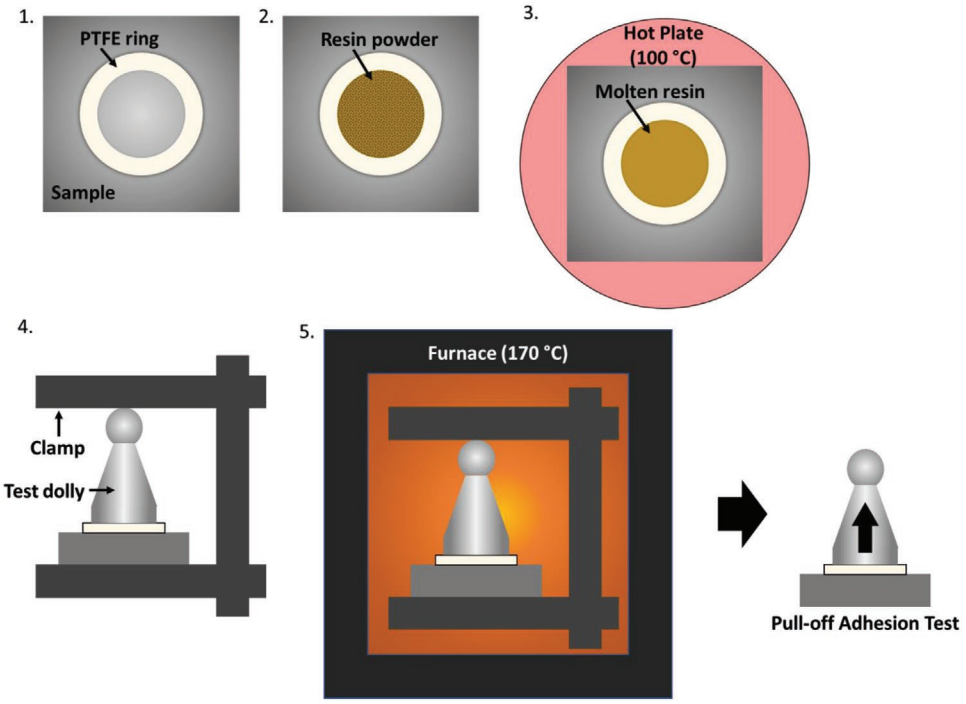

Figure 1. Schematic representation of the procedures for sample preparation for the pull-off tests.

3. Results and Discussions

3.1. Crosslinking Behavior of the Selected Silazanes

The crosslinking behavior of the silazanes PHPS and HTTS has been discussed thoroughly in other studies.[3,6,10,37,38] However, since this behavior is fundamental to understand the influence of temperature on the anti-adherent properties of the coatings, a discussion on this topic is presented herein.

Simplified chemical structures of the selected silazanes are shown in **Figure 2**. In this figure, the chemical groups involved in crosslinking reactions are drawn in red. As mentioned, PHPS (Figure 2a) is a purely inorganic material, composed of a −Si−N− backbone and hydrogen. Both Si−H and N−H bonds are reactive, especially with −OH groups, resulting in an enhanced crosslinking during thermal treatment in air.[6] Durazane 1800—and thus HTTS—contains, additionally to hydrogen, also vinyl and methyl groups attached to the −Si−N− backbone (Figure 2b), hence being called an organosilazane. Due to the lower number of reactive groups, the reactivity of this organosilazane is lower compared to PHPS. In contrast to the methyl groups, vinyl side groups contribute to crosslinking by vinyl polymerization. However, because the onset temperature of these reactions is high,[38] evaporation of molecules with low molecular weight occurs before vinyl polymerization starts, evidenced by mass loss at low temperatures. The addition of the initiator DCP reduces this onset temperature, resulting in a faster crosslinking and a reduced mass loss.[13]

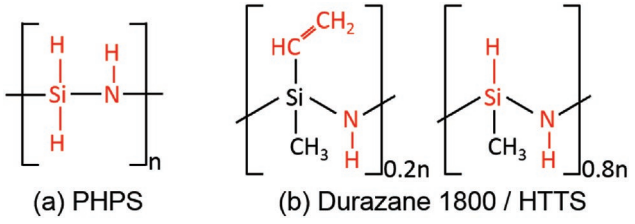

Figure 2. Simplified chemical structure of the selected silazanes. Chemical groups involved in crosslinking reactions are drawn in red.

Thermal conversion of the selected silazanes was investigated by Günthner et al. using thermogravimetric analysis (TGA).[10] Their investigations revealed that both PHPS and HTTS have an outstanding thermal stability. While HTTS containing 3 wt% of DCP undergoes no mass loss up to about 400 °C in air, the mass of PHPS actually increases, because oxygen substitutes hydrogen and nitrogen in the molecular structure of PHPS. An elevated thermal stability is crucial for the application as mold release coating in warm pressing procedures for two main reasons. The first is the fact that the coatings must withstand the temperatures of the CFRP shaping processes without mass loss to avoid damage/contamination of the shaped parts. The second reason is related to the coating's surface. Because mass loss is usually associated with the formation of pores and cavities, the contribution of mechanical interlocking to the overall adhesion of the resin to coated molds increases, and the system loses performance.[24]

The effect of the temperature on crosslinking of the selected silazanes was investigated by FTIR. The wavenumbers of typical bands of silazanes are listed in **Table 1**.[3] These bands are characteristic for the functional groups and the respective bonds in the precursors, such as N−H, C−H, Si−H, Si−CH_3, Si−N−Si, and bonds resulting from crosslinking reactions, e.g. Si−O−Si and Si−CH_2−CH_2−Si.

Table 1. Overview of typical absorption bands of silazanes before and after crosslinking in air[3].

Wavenumber [cm^{-1}]	Vibration band/mode	Wavenumber [cm^{-1}]	Vibration band/mode
3400, 3380	N–H/stretching	1170, 1167	N–H/deformation
3963, 2950	C(sp^3)–H/stretching	1200-1000	Si–O–Si/stretching
2905, 2870	C(sp^3)–H/stretching	1020-820	Si–N–Si, Si–C–Si
2160, 2090	Si–H/deformation	989	Si–CH_2–CH_2–Si
1390, 1370	–CH_3/deformation	912	Si–H/deformation
1266, 1250	Si–CH_3/deformation	800-790	Si–O–Si/stretching

The infrared spectra of PHPS and HTTS after crosslinking at 200 and 300 °C in air are presented in **Figure 3**. The samples are identified by the coating material and the temperature of crosslinking. For example, PHPS_200 corresponds to a PHPS coating crosslinked at 200 °C. Although a distinction of FTIR bands within the fingerprint region (below 1250 cm^{-1}) is difficult, important information is obtained at higher wavenumbers. The spectrum of PHPS (Figure 3a) after crosslinking at 200 °C in air contains a band at about 2180 cm^{-1}, related to deformation of Si—H bonds, which disappears when the temperature during crosslinking is increased to 300 °C. Around 3380 cm^{-1} (stretching of N—H bonds) a very weak band was still detected after treatment at 200 °C, which disappears after treatment at 300 °C. A similar behavior is observed with HTTS (Figure 3b). After thermal treatment at 200 °C, a relatively intense band around 2900 cm^{-1} was measured, corresponding to the stretching of C—H bonds. The absorption band of Si—H bonds is also present. While the latter completely disappears after treatment at 300 °C, the former is still detectable.

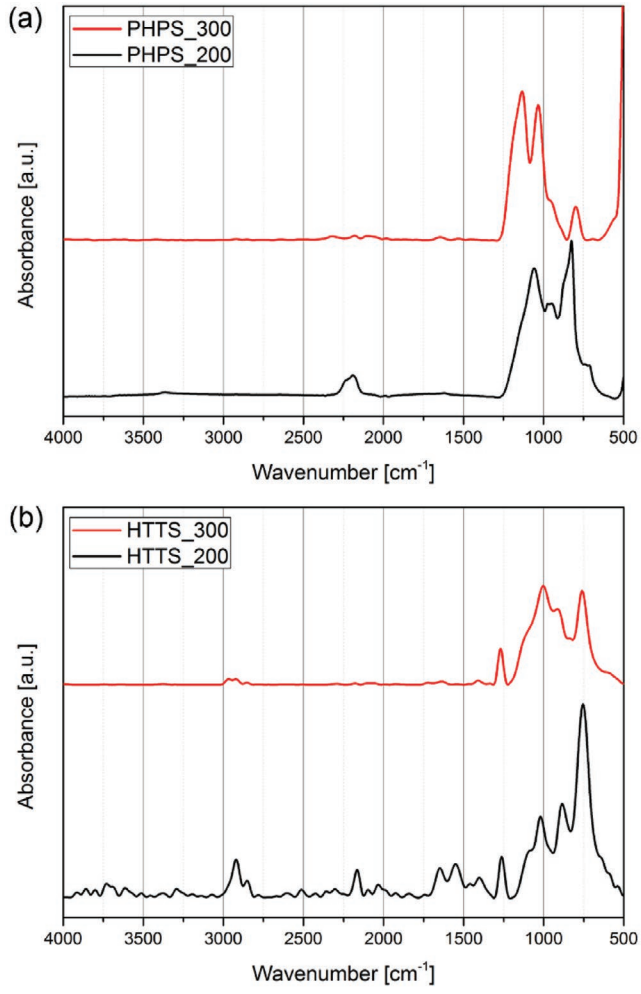

Figure 3. ATR-FTIR spectra of a) PHPS and b) HTTS after crosslinking at 200 and 300 °C in air.

The disappearance of Si—H and N—H bands is explained by the progress of crosslinking reactions, such as dehydrocoupling and transamination, according to Equations (1) and (2), as well as hydrolysis reactions due to moisture in the air (Equation (3)), resulting in the elimination of ammonia and of hydrogen attached to nitrogen atoms[3]

$$\text{Dehydrocoupling}: \quad \equiv Si-H + = N-H \rightarrow \equiv Si-N = + H_2 \uparrow \tag{1}$$

$$\text{Transamination}: 3 \equiv Si-NH-Si \equiv \rightarrow 2N(Si \equiv)_3 + NH_3 \uparrow \tag{2}$$

$$\text{Hydrolysis}: \equiv Si-NH-Si \equiv + H-O-H \rightarrow \equiv Si-O-Si \equiv + NH_3 \uparrow \tag{3}$$

3.2. Coatings without Fillers

First, unfilled coatings were investigated regarding the adhesion of the phenolic resin and other fundamental aspects. These coatings were deposited by dip coating, resulting in layers with a thickness of about 1 µm. Despite the low thickness, stylus profilometry measurements have shown, that the coatings can level the surface considerably, reducing the average R_a roughness from ≈0.4 to values below 0.2 µm (**Figure 4**). This reduction of the surface roughness has a positive effect on the anti-adherent properties. Considering the standard deviation,

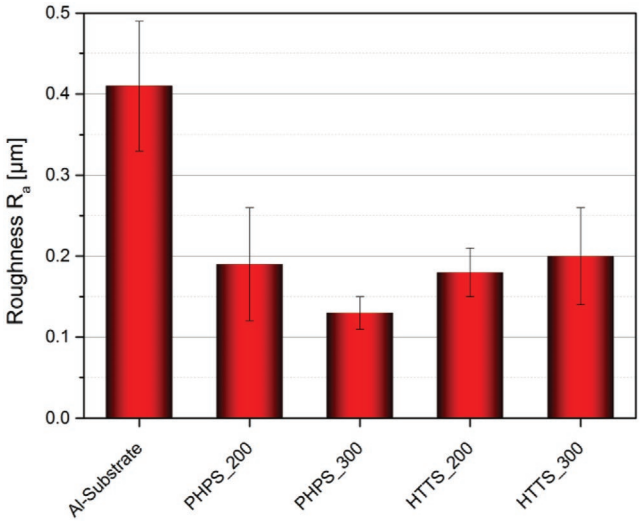

Figure 4. Average roughness R_a of uncoated and coated substrates measured by stylus profilometry. Coatings of PHPS and HTTS after crosslinking at 200 or 300 °C in air.

Table 2. Contact angles of uncoated and coated substrates with water and diiodomethane measured by drop-shape analysis, with the respective surface free energies calculated using the OWRK model. Coatings of PHPS and HTTS after crosslinking at 200 or 300 °C in air.

Surface	CA_{H_2O}	$CA_{CH_2I_2}$	γ_s [mN m^{-1}]	γ_s^{disp} [mN m^{-1}]	γ_s^{pol} [mN m^{-1}]
Al-substrate	57.3° ± 3.6°	54.7° ± 2.3°	49.0 ± 3.7	31.6 ± 1.3	17.4 ± 2.4
PHPS_200	79.4° ± 1.8°	48.0° ± 0.5°	40.0 ± 0.9	35.4 ± 0.3	4.6 ± 0.7
PHPS_300	71.7° ± 0.3°	47.6° ± 0.8°	43.4 ± 0.6	35.6 ± 0.4	7.8 ± 0.2
HTTS_200	86.8° ± 0.4°	49.8° ± 0.6°	36.8 ± 0.5	34.4 ± 0.3	2.4 ± 0.1
HTTS_300	77.5° ± 0.8°	48.8° ± 1.0°	40.4 ± 0.9	34.9 ± 0.6	5.5 ± 0.4

little difference between coatings treated at 200 or 300 °C was measured, which is probably related to relatively high coating thickness compared to the roughness of the substrate.

The measured CA with water and diiodomethane as well as the calculated surface free energies of the unfilled coatings are presented in **Table 2**. As expected, the coatings reduce the SFE of the aluminum substrates from about 49 to less than 43 mN m^{-1}. While the uncoated aluminum substrate has a relatively high polarity—polar component of the surface free energy γ_s^{pol} = 17.4 ± 2.4 mN m^{-1}—the polysilazane coatings are considerably less polar, with the polar component of the SFE being below 8 mN m^{-1}. This means that the wetting of the coated substrates by polar liquids, such as the molten phenolic resin, is worse compared to the uncoated substrates. However, the dispersive component of the SFE increases from 31.6 ± 1.3 mN m^{-1} for the aluminum substrate to values above 34 mN m^{-1} for the polysilazanes. In contrast to the expectations based on the literature,[20] the polysilazane coatings are slightly hydrophilic—, i.e., contact angle with water smaller than 90°—even after treatment at a temperature as low as 200 °C. According to Wang et al.,[20] the surface free energy of polysilazane coatings treated in air is determined by their oxidation state. In the case of PHPS coatings treated at low temperatures (below 300 °C), low SFE and surface polarity result from the Si—H bonds present in the starting material. Despite the fact that oxidation starts at temperatures as low as 100 °C,[3] Si—H bonds still seem to be predominant at the surface. However, during thermal treatment in air at temperatures above 300 °C, oxidation advances, and oxygen-containing groups, such as Si—OH or Si—O—Si, begin to dictate the surface properties. These groups increase the surface polarity as well as the overall SFE. The investigations of Wang and colleagues also led to the conclusion that the highly polar Si—OH groups are likely to dominate after treatment at intermediary temperatures, whereas condensation of these groups at higher temperatures leads to predominantly Si—O—Si at the surface, which are less polar than the silanol groups. Hence, the polarity of the surface and the SFE decrease again in a more advanced oxidation state, although they are still much larger than the values obtained after treatment below 300 °C.

The discrepancy between the values measured by Wang et al. and those obtained in the present study probably arises from different conditions during the thermal treatment. Polysilazanes are reactive in the presence of humidity, leading to a faster incorporation of oxygen into the polymer. In neither of the studies air with a predetermined humidity was used. Thus, different amounts of moisture in the furnace atmosphere may have led to surfaces with different properties, even for samples treated at the same temperature.

Another important factor to consider when comparing the present results with those of Wang and colleagues is the influence of the surface roughness. Ideally, the SFE should be determined onto perfectly flat surfaces. However, those are virtually impossible to achieve. The theories of Wenzel and Cassie–Baxter describe the effects of the surface roughness on the contact angles.[39,40] These theories, which are supported by experimental observations, postulate that the surface roughness amplifies the effects of the surface chemistry. This means that a flat hydrophobic surface becomes more hydrophobic (i.e., the CA with water increases) if the roughness is increased, whereas a flat hydrophilic surface becomes more hydrophilic (i.e., the CA with water decreases) with higher surface roughness. Different contact angles for the same material and liquids, caused simply by different surface roughness, will result in different SFE as well, which may be misinterpreted as a change in surface chemistry. Despite the fact that the authors used sandpaper with the same grit used in the present study (1200) to prepare the surfaces for coating, different substrates—they used a nickel-based alloy—may lead to different values of surface roughness. In addition, the coating thicknesses might have been different as well, leading to different topographies. Thus, a slight change in surface chemistry due to different conditions during thermal treatment may have been amplified by the surface roughness, leading to considerably different results.

In good agreement with the theory provided by Wang et al., the increase of the temperature for the thermal treatment from 200 to 300 °C caused an increase of the SFE and its polar contribution, because of a more advanced incorporation of oxygen into the polymer. Moreover, lower SFEs were obtained with HTTS coatings under the applied conditions. These results were expected based on the composition of the polysilazanes. While PHPS is highly reactive with moisture, due to the presence of a great amount of Si—H and N—H bonds, HTTS has a lower reactivity with moisture, owing to the presence of unreactive methyl and vinyl side groups. Thus, a lower polarity and overall SFE was expected for these coatings.

Adhesion of the coatings to the substrates was investigated by cross-cut tape test, according to the DIN EN ISO 2409. The silazane coatings performed well and no adhesion failure was observed. Thus, coatings were classified as Gt 0, corresponding to the best result possible (**Figure 5**). The grid lines are well defined, and no coating spalling is observed when the tape was stripped off.

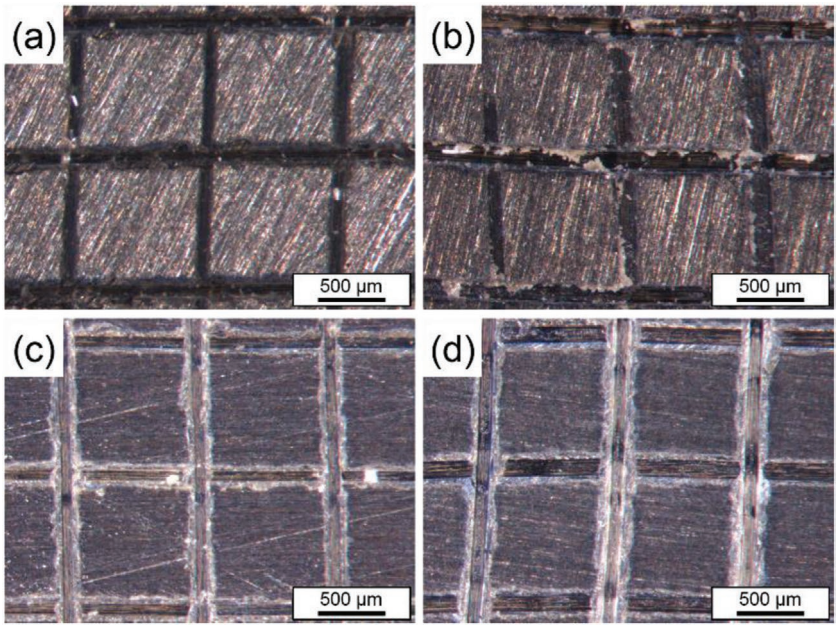

Figure 5. Unfilled polysilazane coatings on aluminum substrates after cross-cut tape test: a) PHPS coating after curing at 200 °C; b) PHPS coating after curing at 300 °C; c) HTTS coating after curing at 200 °C; d) HTTS coating after curing at 300 °C.

It is well known that silazanes adhere to most surfaces, especially metallic, through chemical mechanisms involving the formation of oxygen bridges between surface and the silazane polymer chain.[4,5] The first step of the adhesion mechanism is the wetting of the substrate, to insure an intimate contact between the coating material and the surface. Due to the low surface tension of the liquid coating solution, a good wetting onto the aluminum substrates was expected. The formation of the oxygen bridges occurs by three different mechanisms. The first mechanisms consists in the reaction of Si—H groups with the —OH groups at the surface of the substrate (**Figure 6**a1).[42] In this case, the oxygen bridge is formed upon elimination of hydrogen gas (Figure 6a2) and is not associated to a rupture of the silazane main chain. The second mechanism begins with the rupture of a Si—N bond in the silazane chain (≡Si—NH—Si≡) caused by the interaction with the —OH groups at the surface of the substrate[4] (Figure 6b1). The hydrogen of the hydroxyl group at the surface of the substrate is transferred to the resulting ≡Si—NH group, and the oxygen atom bonds to the silicon separated from the nitrogen (Figure 6b2). In a following step, the bond between silicon and nitrogen in the formed ≡Si—NH_2 group is broken and the hydrogen of another hydroxyl in the vicinity is transferred to the —NH_2 group, forming ammonia, which is released in the process. Silicon then bonds to the remaining oxygen at the surface, forming a second oxygen bridge with the metal (Figure 6b3). Finally, the third mechanism involves hydrolysis of the silazane polymer chain (Figure 6c1), leading to the formation of silanol groups (Si—OH), which react with —OH groups present at the surface of most substrates[5,41] (Figure 6c2), leading to the formation of the oxygen bridges and release of water (Figure 6c3). As discussed in Section 3.1, such reactions occur not only at the interface with the substrate, but also at the surface and within the coating. Thus, water molecules from the atmosphere are unlikely to reach the interface of the coating with the substrate to form the oxygen bridges. However, water molecules adsorbed at the surface of the substrate before coating deposition are easily available and lead to the formation of the oxygen bridges by hydrolysis reactions.

Adhesion of the phenolic resin to the silazane coatings was quantified by pull–off tests (ASTM D4541) using the phenolic resin instead of the usual epoxy resin as an adhesive. The resulting mean pull-off adhesion values are plotted in **Figure 7**. The phenolic resin adheres relatively strongly to the uncoated aluminum substrates, reaching a mean pull-off adhesion of 12.7 MPa. Phenolic resins adhere to aluminum substrates by two main mechanisms. One mechanism is mechanical interlocking. In this case, the molten resin infiltrates surface asperities and then hardens, creating a mechanical bond between substrate and resin. However, since the surface roughness of the used substrates is low (R_a = 0.4 µm), the contribution of mechanical interlocking to the total apparent adhesion is probably low. Another possible adhesion mechanism is by hydrogen bonds between the oxides on the passivating layer of aluminum and —OH groups of the phenolic resin.[43] Also in this case, the surface roughness has an important contribution, since it increases the interfacial contact area. Another important aspect related to the adhesion of the resin to the substrate is the wettability of aluminum. Due to the relatively high SFE of the aluminum substrate, the molten resin can wet the surface well, improving adhesion.

An increase on resin adhesion strength to mean values above 16 MPa is observed when substrates are coated with PHPS, despite the lower SFE of PHPS coatings up to 300 °C, when compared to the substrate. This strong adhesion can be attributed to chemical interactions between coating and resin. As previously discussed, interactions between N—H and Si—H groups of the silazane and —OH groups at the surface of the substrate are responsible for the adhesion of silazanes to most substrates. Since the phenolic resin contains a large amount of —OH groups, a similar adhesion mechanism is expected. Although part of the reactive groups of the silazane disappears due to oxidation and crosslinking reactions during the curing process of the coatings, as suggested by the FTIR measurements and contact angle analyses, a sufficient amount of these groups may still be present, leading to a strong adhesion of the resin to the coating. The fact that the mean adhesion strength of the phenolic resin to the PHPS coatings treated at 300 °C is slightly higher than of the samples treated at 200 °C is in good agreement with contact angle analyses, which revealed higher values of SFE and polarity on the former. These results suggest that the improved surface wettability of the coating treated at 300 °C can somewhat compensate for the disappearance of part of the reactive groups in the polysilazane.

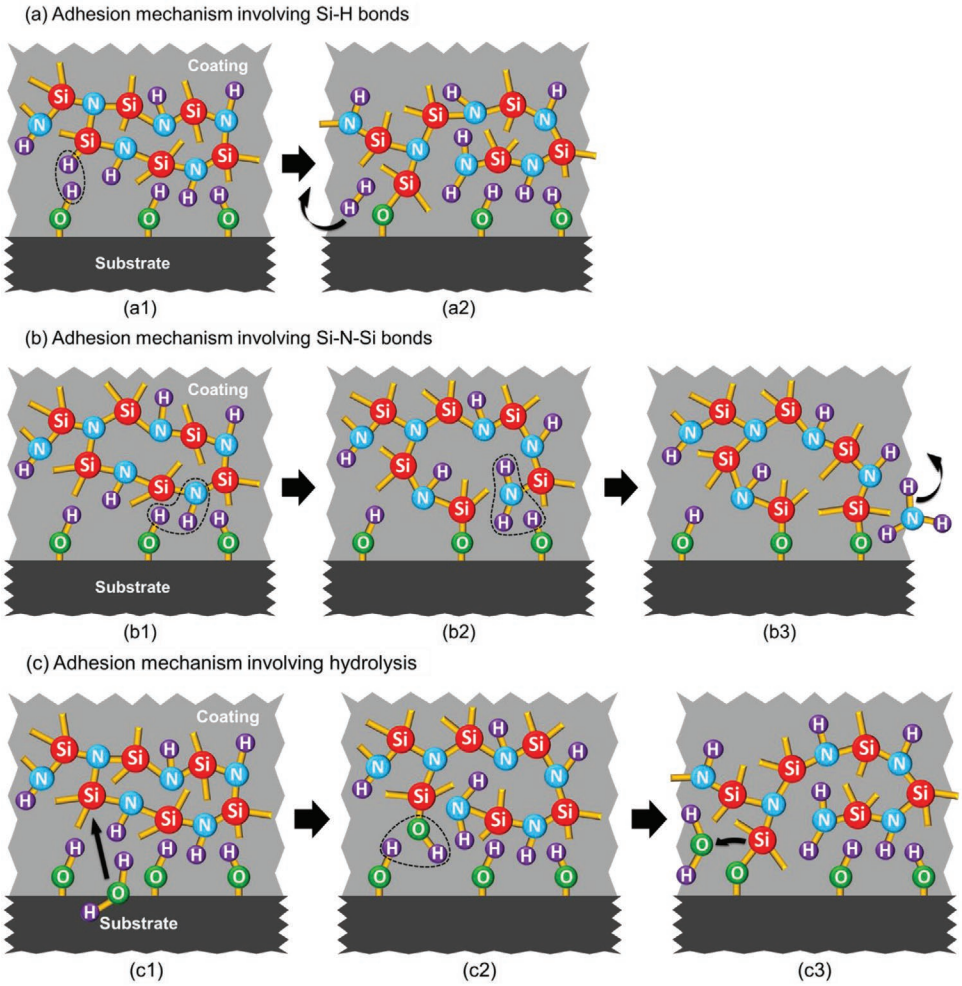

Figure 6. Adhesion mechanisms of silazane coatings, based on Amouzou et al. and Picard et al.[4,5] a) Mechanism involving Si—H bonds: a1) wetting and interaction of —OH groups at the substrate's surface with ≡Si—H groups of the silazane; a2) reaction between ≡Si—H and —OH groups at the substrate's surface and formation of an oxygen bridge with elimination of hydrogen gas. b) Mechanism involving Si—N—Si bonds: b1) wetting and interaction of —OH groups at the substrate's surface with = N—H groups of the silazane; b2) reaction between =N—H groups of the silazane with —OH groups at the substrate's surface, leading to a rupture of the silazane chain and formation of an oxygen bridge and of a Si—NH_2 group; b3) reaction between the —NH_2 group of the silazane with an —OH group at the substrate's surface, forming another oxygen bridge by release of ammonia. c) Mechanism involving hydrolysis: c1) wetting and hydrolysis of the polymer chain by water adsorbed at the substrate's surface, forming a silanol group; c2) interaction between the formed silanol group and —OH groups at the substrate's surface; c3) formation of an oxygen bridge with release of water.

A different behavior is observed with HTTS coatings. In this case, the adhesion strength of the phenolic resin reduces to values around 10 MPa. The difference between PHPS and HTTS coatings is the reduced amount of reactive groups and the presence of organic side groups in the latter, which reduce the interactions of the surface with the resin.[24] Similarly to the PHPS coatings, the mean adhesion value increases only slightly when the temperature during thermal treatment is increased from 200 to 300 °C, as the organic groups remain in the polymer structure.

A qualitative analysis of the tested samples enables an evaluation of the failure mechanism. System failure may occur in five different regions: adhesion failure at the interface substrate/coating, cohesion failure within the coating, adhesion failure at the interface coating/resin, cohesion failure within the resin, and adhesion failure at the interface resin/dolly. Failure may also occur in more than one region. Notwithstanding, for an easy release coating system, failure only at the interface coating/resin is desired, in order to avoid damage of coating and CFRP composite during processing.

An uncoated Al-sample after pull-off test is presented in **Figure 8**. As it would be expected, since both dolly and substrate are made of similar materials, the pull-off test resulted in adhesion failure both at the interfaces substrate/resin (region A) and resin/dolly (region B), with cohesion failure within the resin in the transition of one interface to the other (region C). However, the region corresponding to adhesion failure at the interface substrate/resin (region A) is significantly larger than at the interface resin/dolly (region B), attributed to the rougher surface of the dolly, which improves adhesion.

A somewhat different failure mechanism was observed with the PHPS-coated samples (**Figure 9**). In contrast to uncoated

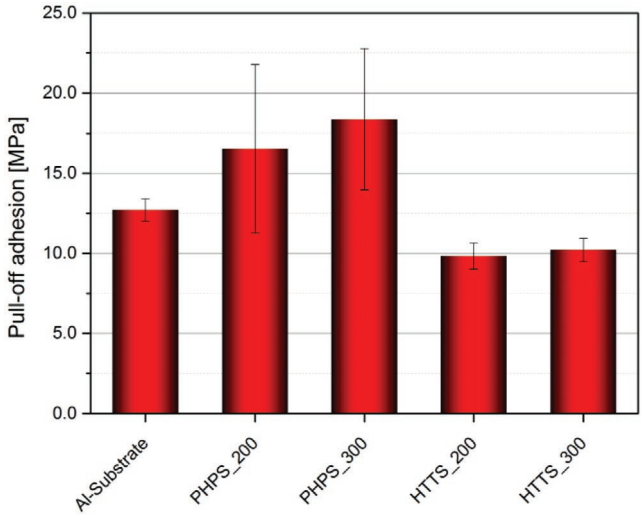

Figure 7. Average pull-off adhesion of the phenolic resin onto uncoated and coated aluminum substrates. Coating crosslinking at 200 or 300 °C in air, resin crosslinking at 170 °C in air.

substrates, no significant adhesion failure occurs at the resin/dolly interface, despite the higher pull-off adhesion. This may be related to the manual preparation of the dolly surface for the pull-off tests, which in this case led to a stronger adhesion. Two distinct regions were identified after pull-off tests. The first (region A) corresponds to adhesion failure at the interface coating/resin. The second (region B), which is predominant, corresponds to cohesion failure within the resin, evidencing the strong adhesion of the resin to the coating and to the dolly. This predominant cohesion failure within the resin explains also the variation of the adhesion values (Figure 7). Since the failure of the system is dependent on crack propagation within the resin, the presence of pores and defects should lead to lower pull-off adhesion values, whereas defect free resin layers should lead to higher pull-off adhesion values. It is also important to mention the correlation between failure mechanism and crosslinking temperature. The region corresponding to adhesion failure between coating and resin (region A) is smaller for coatings crosslinked at 300 °C, evidencing a stronger interfacial adhesion between coatings treated at 300 °C and the resin. These results are in good agreement with the quantitative analyses,

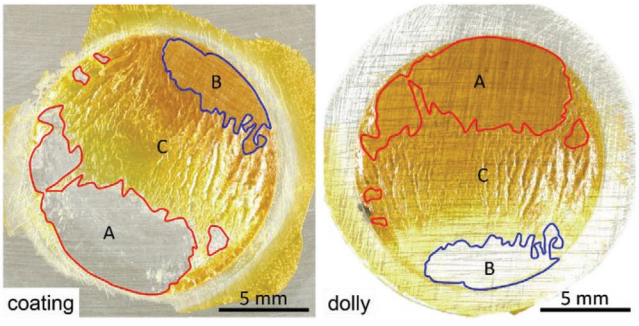

Figure 8. Digital images of an uncoated substrate and the respective dolly after pull-off test. Region A: adhesion failure at the interface substrate/resin; region B: adhesion failure at the interface resin/dolly; and region C: cohesion failure within the resin layer. Resin crosslinking at 170 °C in air.

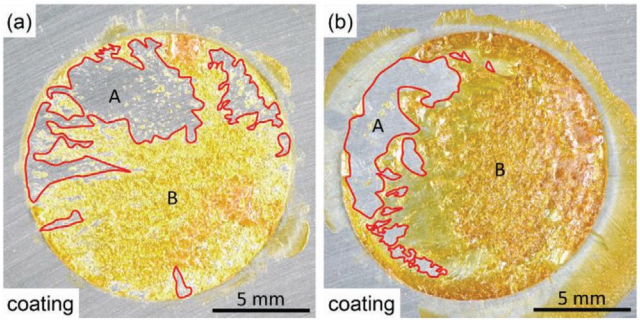

Figure 9. Digital images of samples with PHPS coatings crosslinked at a) 200 and b) 300 °C after pull-off test. Region A: adhesion failure at the interface coating/resin; and region B: cohesion failure within the resin layer. Resin crosslinking at 170 °C in air.

since the mean pull-off adhesion of the resin is slightly higher on coatings crosslinked at 300 °C than onto those treated at 200 °C.

HTTS-coated samples were subjected to the same evaluation as the uncoated and PHPS-coated samples, whereby significant differences became evident (**Figure 10**). When HTTS coatings are applied, predominantly adhesion failure at the interface coating/resin occurs. Although the damage to the resin layer is not extensive, a small amount of resin remains adhered to the coating. Similarly to the quantitative analyses, no significant differences between coatings crosslinked at 200 or 300 °C were observed.

Based on the presented results, HTTS was selected as precursor for the development of particle-filled anti-adherent coating systems, to reduce further the adhesion of the phenolic resin to the coated substrates.

3.3. Coatings with Fillers

Three different materials were investigated as fillers in HTTS-based coatings—graphite, hexagonal boron nitride and PTFE—in volume fractions ranging from 5 to 70 vol%. Graphite and h-BN lead to rough surfaces with pores and cavities, which result in a stronger adhesion of the phenolic resin. As a consequence, cohesion failure within the coating occurs and coating material remains adhered to the phenolic resin after pull-off

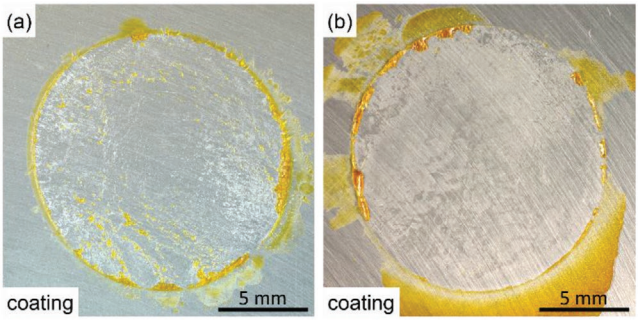

Figure 10. Digital images of samples with HTTS coatings crosslinked at a) 200 and b) 300 °C after pull-off test. Region A: adhesion failure at the interface coating/resin; and region B: cohesion failure within the resin layer.

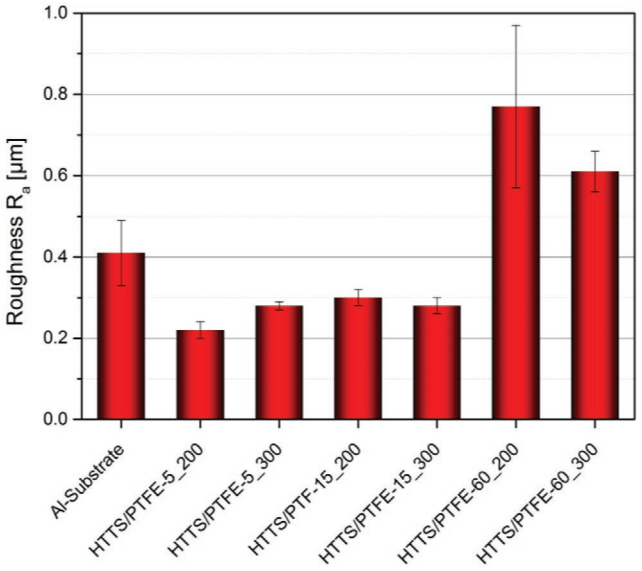

Figure 11. Average roughness R_a of uncoated and coated substrates (polished) measured by stylus profilometry. Coatings of HTTS/PTFE with different amounts of PTFE, after crosslinking at 200 or 300 °C in air.

tests. While residues of graphite-filled polysilazane coatings should not influence the behavior of the CFRP bodies during pyrolysis and LSI processes significantly, the contamination with h-BN is detrimental. In the case of the manufacturing of plastic parts not intended for pyrolysis, any contamination of the surface is an issue. Moreover, the removal of coating material leads to a short lifespan of the coatings, demanding frequent reapplication and increasing processing costs. Hence, for the sake of brevity, these coatings are not further discussed in this paper.

PTFE-filled coatings were prepared with filler amounts ranging from 5 to 70 vol%, with steps of 5 vol%. Three representative model systems were selected for discussion in this paper: 5, 15, and 60 vol%. The different systems were named according to the composition and crosslinking temperature. For example, HTTS/PTFE-5_200 corresponds to a coating system composed of HTTS and PTFE, with 5 vol% of PTFE, and crosslinking temperature of 200 °C.

A small reduction of the surface roughness compared to the uncoated substrates is achieved with coatings containing low amounts of filler (**Figure 11**)—R_a decreases from 0.4 to less than 0.3 µm. With higher filler fractions, however, surface roughness increases considerably (R_a above 0.6 µm). This is because the precursor amount is too low to form a continuous matrix to embed the particles near the surface, creating a rougher surface.

All PTFE-filled coatings, in contrast to systems with graphite and h-BN, have a relatively smooth surface, as evidenced by SEM analyses (**Figure 12**). However, a PTFE amount below 15 vol% leads in some cases to cracking of the coatings during curing at 300 °C—all coatings were applied with the same deposition parameters. This crack formation can be attributed to the shrinkage of the precursor, caused by a density increase. Günthner et al.[3] have shown that silazanes can undergo a volume shrinkage above 20% upon thermal

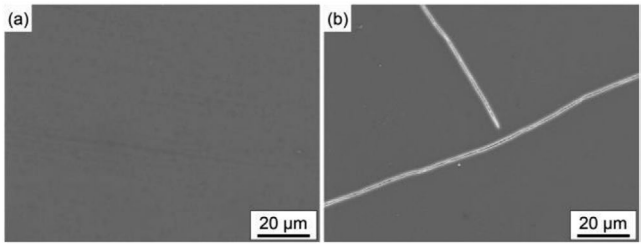

Figure 12. SEM micrographs of the surface of coatings: a) HTTS/PTFE-5 after crosslinking at 200 °C, b) HTTS/PTFE-5 after crosslinking at 300 °C.

treatment up to 300 °C in air. However, this shrinkage is constrained by the adhesion to the substrate, generating tensile stress within the coatings.[44] With a reduced filler amount, precursor shrinkage becomes more relevant, whereby the critical coating thickness is reduced. The critical coating thickness is the thickness, above which the tensile stresses cause the formation of segmentation cracks (across the thickness),[44] as shown in Figure 12 for coatings with 5 vol% PTFE. Moreover, also the coefficient of thermal expansion (CTE) may have an influence on crack formation. Due to its high CTE,[45] PTFE is able to compensate, at least partially, precursor's shrinkage and increase the overall CTE of the coating system. Thus, the expansion mismatch compared to the aluminum substrate during thermal treatment is reduced, which also reduces the stresses arising within the coatings. Due to the lower critical thickness, systems with less than 15 vol% of PTFE demand a more precise control during deposition, becoming less suitable for large-scale applications, especially for complex shapes and manual spray deposition.

The contact angle analyses of the PTFE-filled coating systems led to interesting findings (**Table 3**). As expected, the SFE decreases as the amount of PTFE in the system is increased. SFE values as low as 3–4 mN m^{-1} are achieved with 60 vol% PTFE particles mixed with HTTS. This is because a higher amount of particles increases the probability that particles will be located at the surface of the coating. With more PTFE particles at the surface, the surface properties tend to approach the characteristics of pure PTFE, with a low SFE (≈18 mN m^{-1} for a smooth surface) and polarity close to zero.[46] Remarkably, even an amount of PTFE particles as low as 5 vol% leads to a reduction of the SFE compared to the pure HTTS coatings from values above 40 mN m^{-1} to values below 37 mN m^{-1}. Moreover, the surface roughness clearly influences the CA measurements (Figure 11), since CA with water of the systems containing 60 vol% PTFE are higher than the typical values for a smooth surface of pure PTFE (≈117°[46]).

According to the results, the SFE of the systems containing PTFE depends on the temperature of the thermal treatment. For the system containing 5 vol% PTFE after treatment at 200 °C, the CA with water was measured to be around 85°, about 58° with diiodomethane, and the SFE amounts to about 33 mN m^{-1}. After treatment at 300 °C, the CA with water decreases to about 78°, the CA with diiodomethane remains virtually unchanged, and the SFE increases to 37 mN m^{-1}. The difference in the values of SFE and CA with water is attributed to the increase of the polarity of the surface, which raises from about 4 to almost 7 mN m^{-1}, increasing the affinity of the

Table 3. Contact angles with water and diiodomethane of the coatings containing PTFE particles as filler after crosslinking at 200 or 300 °C in air. Contact angles measured by drop-shape analysis and surface free energies calculated using the OWRK model. Values for the aluminum substrate and HTTS coatings for comparison.

Surface	CA_{H_2O}	$CA_{CH_2I_2}$	γ_s [mN m^{-1}]	γ_s^{disp} [mN m^{-1}]	γ_s^{pol} [mN m^{-1}]
Al-substrate	57.3° ± 3.6°	54.7° ± 2.3°	49.0 ± 3.7	31.6 ± 1.3	17.4 ± 2.4
HTTS_200	86.8° ± 0.4°	49.8° ± 0.6°	36.8 ± 0.5	34.4 ± 0.3	2.4 ± 0.1
HTTS_300	77.5° ± 0.8°	48.8° ± 1.0°	40.4 ± 0.9	34.9 ± 0.6	5.5 ± 0.4
HTTS/PTFE-5_200	85.3° ± 0.9°	58.2° ± 0.2°	33.5 ± 0.5	29.6 ± 0.1	3.8 ± 0.3
HTTS/PTFE-5_300	77.9° ± 0.5°	57.5° ± 0.6°	36.7 ± 0.6	30.0 ± 0.3	6.7 ± 0.2
HTTS/PTFE-15_200	110.8° ± 0.6°	72.6° ± 2.0°	21.5 ± 1.1	21.4 ± 1.1	0.1 ± 0.0
HTTS/PTFE-15_300	89.5° ± 1.5°	54.4° ± 1.4°	33.9 ± 1.2	31.8 ± 0.8	2.1 ± 0.4
HTTS/PTFE-60_200	144.6° ± 5.3°	119.3° ± 1.3°	3.4 ± 0.4	3.3 ± 0.3	0.1 ± 0.1
HTTS/PTFE-60_300	135.4° ± 2.2°	115.6° ± 2.4°	4.1 ± 0.6	4.1 ± 0.6	0.0 ± 0.01

surface with water (polar liquid). Similar effects on the contact angle with water were observed with the systems containing 15 and 60 vol% PTFE. However, the polarity of these surfaces was much lower—which is consistent with the properties of PTFE. The polar component of the SFE of samples containing 15 vol% PTFE increases from practically zero after treatment at 200 °C, to ≈2 mN m^{-1} after curing at 300 °C. However, the SFE increases mostly due to a significant increase of the dispersive component, from ≈21 mN m^{-1} after crosslinking at 200 °C, to almost 32 mN m^{-1} after the treatment at 300 °C. The changes of the surface properties of coatings containing 60 vol% PTFE were much more subtle. While the polar component remained near zero after treatment at both temperatures, the dispersive component increases only slightly from ≈29 mN m^{-1} after the treatment at 200 °C, to ≈34 mN m^{-1} after crosslinking at 300 °C. The properties of this coating system lead to surfaces with highly hydrophobic and even oleophobic characteristics, with contact angles above 130° with water and above 115° with diiodomethane.

Similarly to the unfilled coatings, PTFE-filled systems perform well in the cross-cut-tape tests (**Figure 13**). Aside from a deformation of the coatings at the borders of the squares due to displacement of aluminum upon scratching the surface, no defects are noticeable, and the coatings could be classified as Gt 0 for both crosslinking temperatures. However, it is important to mention, that the tension applied during stripping of the tape is probably lower as is the case for the unfilled coatings, due to the lower surface energy of the PTFE-filled coatings, which reduces the adhesion strength of the tape. Nonetheless, scratching the coated samples does not lead to coating failure, thus evidencing the strong adhesion of the developed systems. Moreover, the tape removed from the coatings with 60 vol% PTFE particles becomes more opaque, suggesting the removal of coating material. However, since the substrate is not exposed, one can conclude that only the outermost, loosely attached PTFE particles were removed from the surface.

Adhesion of the phenolic resin to HTTS/PTFE coatings was investigated by pull-off tests (**Figure 14**). A significant improvement is obtained compared to pure HTTS coatings. While the average pull-off adhesion to uncoated substrates and to HTTS coatings amounts to 12.7 and ≈10 MPa, respectively, it remains below 8 MPa for all HTTS/PTFE coating systems. As previously

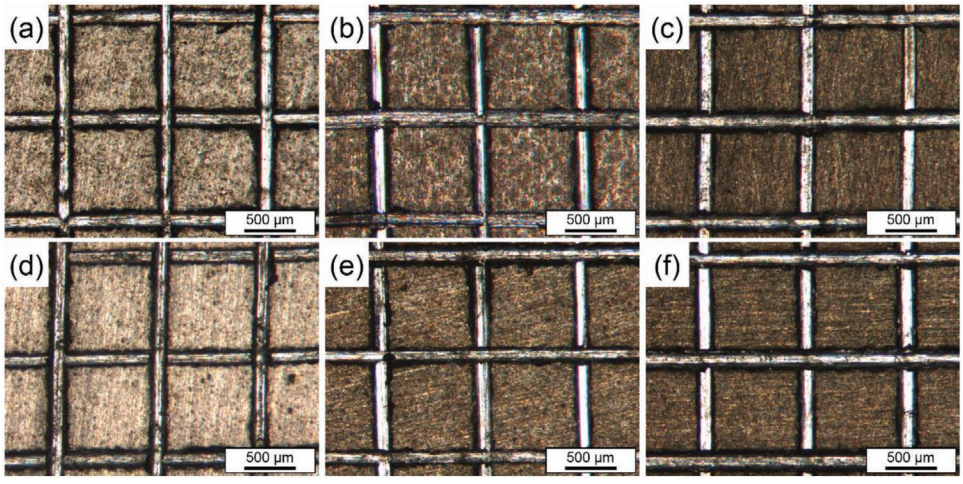

Figure 13. PTFE-filled HTTS coatings on aluminum substrates after cross-cut tape test. Samples cured at 200 °C: a) 5 vol% PTFE; b) 15 vol% PTFE; and c) 60 vol% PTFE; samples cured at 300 °C: d) 5 vol% PTFE; e) 15 vol% PTFE; and f) 60 vol% PTFE.

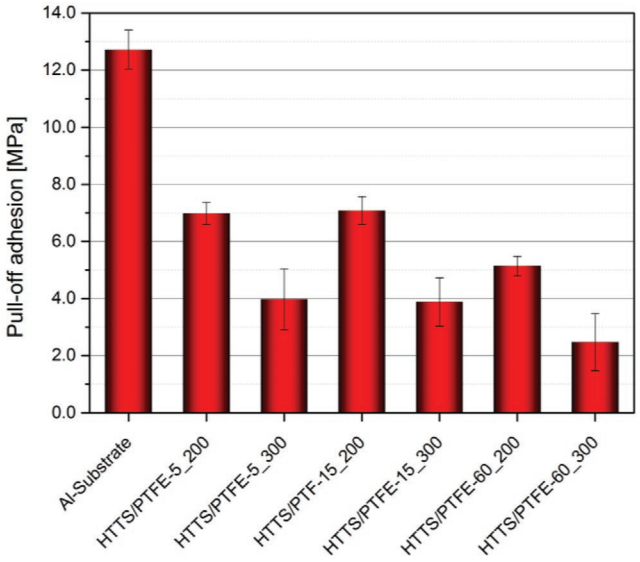

Figure 14. Mean pull-off adhesion of the phenolic resin onto aluminum substrates: uncoated and coated with HTTS/PTFE suspensions containing 5 vol% PTFE, 10 vol% PTFE and 60 vol% PTFE. Coating crosslinking at 200 or 300 °C in air, resin crosslinking at 170 °C in air.

discussed, an increase of the crosslinking temperature from 200 to 300 °C leads to an increase of the SFE, improving the wetting of the surface. In spite of that, the adhesion strength of the phenolic resin to the coatings decreases for all investigated HTTS/PTFE systems. Since this was not the case for pure HTTS coatings, this effect can be attributed to the PTFE filler particles.

The filler amount has a strong influence on the adhesion of the resin to the coatings. Coatings with 5 and 15 vol% PTFE lead to similar pull-off adhesion values: ≈7 MPa after crosslinking at 200 °C and below 4 MPa after crosslinking at 300 °C. Also this result is inconsistent with the contact angle analyses, which revealed a lower SFE of the coatings with 15 vol% compared to the coatings with 5 vol% PTFE treated at the same temperatures. Moreover, the surface roughness of both systems is also similar (Figure 11). Thus, a compensation of lower SFE values, which reduces the adhesion, by higher surface roughness due to a higher amount of filler particles, which would increase the adhesion, was not experimentally observed. The lowest adhesion values for each of the tested crosslinking temperatures were achieved with 60 vol% PTFE particles, with 5.1 and 2.5 MPa for crosslinking temperatures of 200 and 300 °C, respectively. Since the amount of particles is high, it is likely that a larger number of particles is exposed at the surface, hence the SFE is very low. Moreover, loosely attached PTFE particles at the coating surface may be responsible for the weak adhesion of the phenolic resin, as observed after the cross-cut tape tests.

The inconsistency between the values of the adhesion strength of the resin, the contact angle analyses and surface roughness values indicates that the adhesion of the resin is determined not only by the wetting of the surface and mechanical interlocking, but also by the chemical interactions of the resin with the polysilazane during the curing process of the resin. This explains the lower adhesion values onto coatings treated at 300 °C. During the thermal treatment, the reactive groups in HTTS react with each other and with the atmosphere, leading to an increased degree of crosslinking of the polymer network. The higher the temperature during the thermal treatment, the more advanced is the crosslinking process, i.e., less reactive groups remain available for bonding reactions with the resin. Thus, despite the improved wettability of the surface, due to the higher SFE, less chemical interactions between coating and resin after treatment at 300 °C lead to a weaker adhesion of the resin. The fact that the adhesion strength of the resin to the pure HTTS coatings does not change significantly with the change in crosslinking temperature may suggest that the higher SFE and polar component are sufficient to compensate for the weaker chemical interactions of the resin with the pure HTTS coatings but insufficient in the case of the PTFE-filled systems. However, complementary chemical analyses of the surfaces are still required to clarify this issue.

Pull-off test samples were also qualitatively analyzed regarding failure mechanism (**Figure 15**). The occurrence exclusively of adhesion failure at the interface coating/resin is observed for all HTTS/PTFE coatings. Moreover, no significant

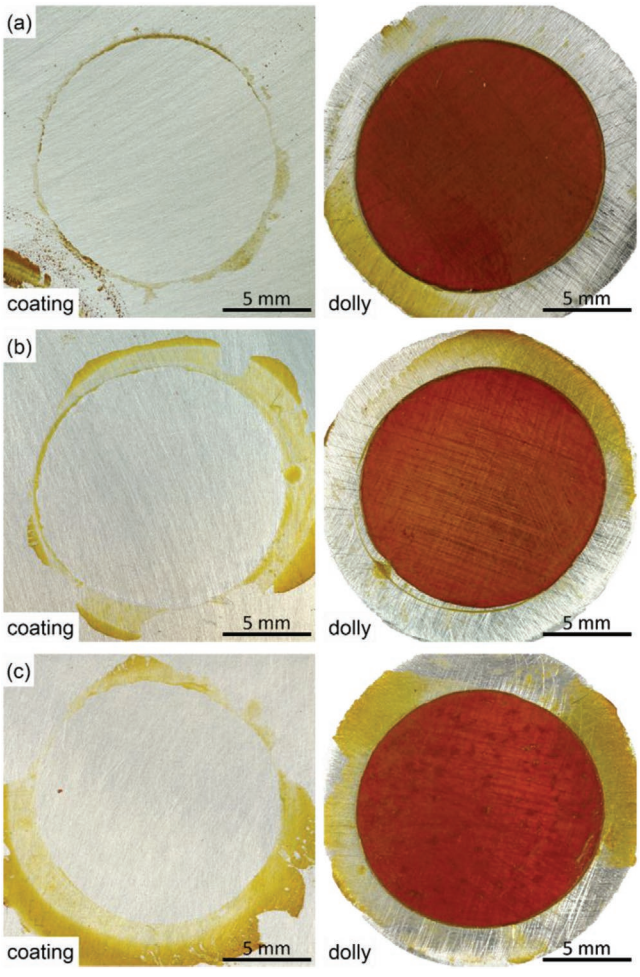

Figure 15. Digital images of surfaces of HTTS/PTFE coatings crosslinked at 300 °C with the respective dollies after pull-off tests: a) 5 vol% PTFE; b) 15 vol% PTFE; and c) 60 vol% PTFE. Resin crosslinking at 170 °C in air.

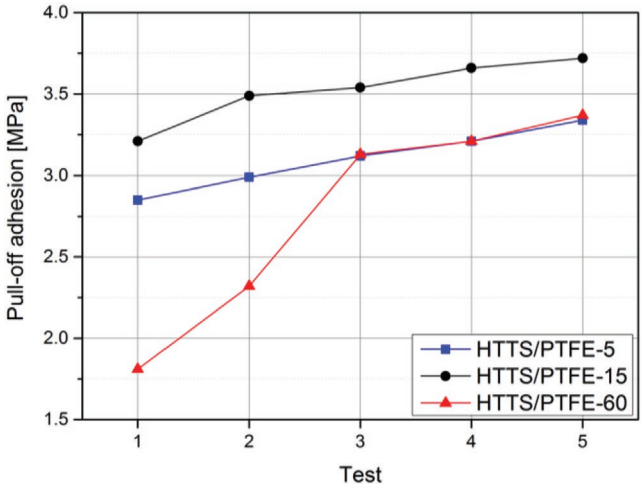

Figure 16. Variation of the adhesion values upon repeated pull-off tests on the same spot of each sample. Coatings of HTTS with 5, 15, and 60 vol% PTFE crosslinked in air at 300 °C. Resin crosslinking at 170 °C.

amount of resin remains adhered to the coatings and the transfer of coating material to the resin was not apparent, although it is expected to occur with the system containing 60 vol% PTFE. These results confirm the applicability of the developed systems as anti-adherent coatings for the warm pressing of the phenolic resin using aluminum molds.

In order to select the best coating systems for the application under production conditions, durability tests were performed. The measured adhesion values are shown in **Figure 16**. Although the anti-adherent properties improve by increasing the amount of filler, the durability of the coatings is most likely reduced, since the silazane is responsible for the cohesion of the coating system. To verify this influence, durability tests were carried out by performing repeated pull-off tests on the same spot of coated Al-samples crosslinked at 300 °C.

Systems with 5 and 15 vol% PTFE showed a slight increase of the resin's adhesion after each test. However, even after five tests, the adhesion strength of the resin to the HTTS/PTFE coatings is still much lower when compared to the uncoated Al-substrate and to the coatings without filler. However, a larger variation of the adhesion values was measured for the system containing 60 vol% of PTFE. As indicated by the cross-cut tape tests, loosely attached PTFE particles are easily removed and transferred from the coating to the resin during pull-off test, reducing the adhesion of the resin. The repetition of the pull-off test on the same area eventually leads to a removal of all loose particles. From this point, the adhesion strength of the resin to the surface increases more mildly and the measured values are similar to those of the systems with a lower amount of PTFE.

It is important to mention that, for industrial applications, coatings with a small amount of PTFE filler are preferred, due to the high costs of PTFE powder. However, crack formation was observed on HTTS coatings with only 5 vol% of PTFE. Thus, the coating system with 15 vol% of PTFE seems to be the most suitable system for this application. This system combines a higher critical coating thickness, with good anti-adherent properties and an excellent durability by repeatedly application. However, systems with lower PTFE amounts may be used in an eventual application in large scale, if the parameters for deposition are optimized and reproducible, to ensure a homogeneous deposition of coatings with thickness below the critical value.

4. Conclusions

Anti-adherent coatings based on two commercially available, chemically different polysilazanes (PHPS, HTTS) were investigated using aluminum as substrate. Coatings were applied by common dip or spray coating methods and treated at two different temperatures (200 and 300 °C) in air. A methodology based on pull-off tests was used to measure the adhesion of a phenolic resin with the different surfaces.

Coatings prepared from the very reactive, inorganic polysilazane PHPS possess a higher SFE after crosslinking at 200 °C in comparison to the coatings based on the less reactive organopolysilazane HTTS. An increase of the temperature to 300 °C causes a further increase of the SFE and its polar component for both precursors, due to the enhanced incorporation of oxygen into the polymer structure. Because of the formation of strong bonds with the phenolic resin, the adhesion strength between the PHPS coatings and the resin amounts to more than 16 MPa in comparison to ≈12 MPa to the uncoated aluminum substrates. In contrast, HTTS coatings reduce the adhesion of the resin to values of about 10 MPa.

To further improve the anti-adherent properties of HTTS-based coatings, PTFE particles were added as filler. Coatings containing different amounts of PTFE particles (5, 15, and 60 vol%) treated at 200 and 300 °C in air were compared. As expected based on the properties of PTFE, the contact angles of the coatings increased up to 145° with water and almost 120° with diiodomethane because of the further reduced SFE and the surface roughness caused by the filler particles. Although the SFE of the PTFE-filled coatings is lower after crosslinking at 200 °C, lower adhesion values of the phenolic resin to the coatings were measured after crosslinking at 300 °C. These results suggest that the higher crosslinking temperature facilitates the reaction of reactive groups in HTTS with each other and with the air moisture, resulting in a lower amount of groups available for reactions with the phenolic resin. A minimum of the pull-off-adhesion of less than 3 MPa was measured for the coating system HTTS with 60 vol% PTFE crosslinked at 300 °C, which is partially attributed to the removal of PTFE particles from the surface, leading to an increase of the adhesion values after repeated pull-off tests. In contrast, the adhesion of the resin to the system containing 15 vol% PTFE in HTTS amounts to values below 4 MPa and remain stable even after repeated tests on the same area. Moreover, using the applied deposition parameters, coatings from this system are crack-free, as opposed to the system containing only 5 vol% PTFE.

The thermal stability and the surface properties of the developed PTFE-containing HTTS coatings are comparable to commercial PTFE coatings, but their application is much simpler as neither pretreatment of the substrate (e.g., roughening) to enable adhesion nor high pressure and annealing at higher temperatures for longer times to form a homogeneous layer are

necessary. In contrast to the physical adhesion of PTFE layers, the precursor layers are chemically bonded to metal substrates.

Acknowledgements

The authors acknowledge the Bavarian Research Foundation (Bayerische Forschungsstiftung) for financial support through the project "ForNextGen—Next Generation Tools (AZ-1117-14), TP4."

Conflict of Interest

The authors declare no conflict of interest.

Keywords

anti-adherent coatings, carbon-fiber reinforced plastics, mold release coatings, polysilazanes, poly(tetrafluoroethylene) (PTFE)

Received: November 20, 2019
Revised: February 26, 2020
Published online: April 15, 2020

[1] P. Colombo, G. Mera, R. Riedel, G. D. Sorarù, *J. Am. Ceram. Soc.* **2010**, *93*, 1805.
[2] G. Barroso, Q. Li, R. K. Bordia, G. Motz, *J. Mater. Chem. A* **2019**, *7*, 1936.
[3] M. Günthner, K. Wang, R. K. Bordia, G. Motz, *J. Eur. Ceram. Soc.* **2012**, *32*, 1883.
[4] D. Amouzou, L. Fourdrinier, F. Maseri, R. Sporken, *Appl. Surf. Sci.* **2014**, *320*, 519.
[5] L. Picard, P. Phalip, E. Fleury, F. Ganachaud, *Prog. Org. Coat.* **2015**, *80*, 120.
[6] F. Bauer, U. Decker, A. Dierdorf, H. Ernst, R. Heller, H. Liebe, R. Mehnert, *Prog. Org. Coat.* **2005**, *53*, 183.
[7] A. Lukacs, *Am. Ceram. Soc. Bull.* **2007**, *86*, 9301.
[8] Y. Naganuma, S. Tanaka, C. Kato, T. Shindo, *J. Ceram. Soc. Jpn.* **2004**, *112*, 599.
[9] L. Prager, A. Dierdorf, H. Liebe, S. Naumov, S. Stojanovic, R. Heller, L. Wennrich, Buchmeiser, *Chem. - Eur. J.* **2007**, *13*, 8522.
[10] M. Günthner, M. Pscherer, C. Kaufmann, G. Motz, *Sol. Energy Mater. Sol. Cells* **2014**, *123*, 97.
[11] G. Barroso, T. Kraus, U. Degenhardt, M. Scheffler, G. Motz, *Adv. Eng. Mater.* **2016**, *18*, 746.
[12] T. Coan, G. S. Barroso, R. A. F. Machado, F. S. de Souza, A. Spinelli, G. Motz, *Prog. Org. Coat.* **2015**, *89*, 220.
[13] M. Günthner, A. Schütz, U. Glatzel, K. Wang, R. K. Bordia, O. Greißl, W. Krenkel, G. Motz, *J. Eur. Ceram. Soc.* **2011**, *31*, 3003.
[14] M. Günthner, T. Kraus, A. Dierdorf, D. Decker, W. Krenkel, G. Motz, *J. Eur. Ceram. Soc.* **2009**, *29*, 2061.
[15] J. Bill, D. Heimann, *J. Eur. Ceram. Soc.* **1996**, *16*, 1115.
[16] M. Lenz Leite, G. Barroso, M. Parchovianský, D. Galusek, E. Ionescu, W. Krenkel, G. Motz, *J. Eur. Ceram. Soc.* **2017**, *37*, 5177.
[17] J. Liu, L. Zhang, J. Yang, L. Cheng, Y. Wang, *J. Eur. Ceram. Soc.* **2012**, *32*, 705.
[18] G. S. Barroso, W. Krenkel, G. Motz, *J. Eur. Ceram. Soc.* **2015**, *35*, 3339.
[19] B. Hoffmann, M. Feldmann, G. Ziegler, *J. Mater. Chem.* **2007**, *17*, 4034.
[20] K. Wang, M. Gunthner, G. Motz, B. D. Flinn, R. K. Bordia, *Langmuir* **2013**, *29*, 2889.
[21] A. Morlier, S. Cros, J.-P. Garandet, N. Alberola, *Thin Solid Films* **2012**, *524*, 62.
[22] V. Bakumov, K. Gueinzius, C. Hermann, M. Schwarz, E. Kroke, *J. Eur. Ceram. Soc.* **2007**, *27*, 3287.
[23] S. Marceaux, C. Bressy, F.-X. Perrin, C. Martin, A. Margaillan, *Prog. Org. Coat.* **2014**, *77*, 1919.
[24] G. W. Critchlow, R. E. Litchfield, I. Sutherland, D. B. Grandy, S. Wilson, *Int. J. Adhes. Adhes.* **2006**, *26*, 577.
[25] R. E. Litchfield, G. W. Critchlow, S. Wilson, *Int. J. Adhes. Adhes.* **2006**, *26*, 295.
[26] S. Rossi, G. Gai, R. de Benedetto, *Mater. Des.* **2014**, *53*, 782.
[27] H. Unal, A. Mimaroglu, U. Kadıoglu, H. Ekiz, *Mater. Des.* **2004**, *25*, 239.
[28] *Polymer Handbook* (Ed: J. Brandrup), 3rd ed., Wiley, New York **1989**.
[29] S. M. Yeo, A. A. Polycarpou, *Tribol. Int.* **2013**, *60*, 198.
[30] D. J. Sordelet, S. D. Widener, Y. Tang, M. F. Besser, *Mater. Sci. Eng., A* **2000**, *294–296*, 834.
[31] Q. Zhao, Y. Liu, H. Müller-Steinhagen, G. Liu, *Surf. Coat. Technol.* **2002**, *155*, 279.
[32] Z. Peng, L. Gang, T. Yangchao, T. Xuehong, *Sens. Actuators, A* **2005**, *118*, 338.
[33] B. Kaynak, C. Alpan, M. Kratzer, C. Ganser, C. Teichert, W. Kern, *Appl. Surf. Sci.* **2017**, *416*, 824.
[34] J. Jiang, Y. Fu, Q. Zhang, X. Zhan, F. Chen, *Appl. Surf. Sci.* **2017**, *412*, 1.
[35] M. Long, S. Peng, W. Deng, X. Yang, K. Miao, N. Wen, X. Miao, W. Deng, *J. Colloid Interface Sci.* **2017**, *508*, 18.
[36] A. J. Shields, D. M. Hepburn, I. J. Kemp, J. M. Cooper, *Polym. Degrad. Stab.* **2000**, *70*, 253.
[37] O. Flores, T. Schmalz, W. Krenkel, L. Heymann, G. Motz, *J. Mater. Chem. A* **2013**, *1*, 15406.
[38] R. Chavez, E. Ionescu, C. Balan, C. Fasel, R. Riedel, *J. Appl. Polym. Sci.* **2011**, *119*, 794.
[39] R. N. Wenzel, *Ind. Eng. Chem.* **1936**, *28*, 988.
[40] A. B. D. Cassie, S. Baxter, *Trans. Faraday Soc.* **1944**, *40*, 546.
[41] W. J. van Ooij, D. Q. Zhu, G. Prasad, S. Jayaseelan, Y. Fu, N. Teredesai, *Surf. Eng.* **2000**, *16*, 386.
[42] G. Motz, T. Schmalz, S. Trassl, R. Kempe, in *Design, Processing and Properties of Ceramic Materials from Preceramic Precursors* (Ed: S. Bernard), Nova Science Publishers Inc, New York **2012**, pp. 15–35.
[43] A. J. Kinloch, *Adhesion and Adhesives*, Chapman & Hall, London **1994**.
[44] R. K. Bordia, R. Raj, *J. Am. Ceram. Soc.* **1985**, *68*, 287.
[45] R. K. Kirby, *J. Res. Natl. Bur. Stand.* **1956**, *57*, 91.
[46] D. H. Kaelble, E. H. Cirlin, *J. Polym. Sci., Polym. Phys. Ed.* **1971**, *9*, 363.